



# Transport of FNPP1-derived radiocaesium from subtropical mode water in the western North Pacific Ocean to the Sea of Japan

Yayoi Inomata<sup>1</sup>, Michio Aoyama<sup>2</sup>, Yasunori Hamajima<sup>1</sup>, and Masatoshi Yamada<sup>3</sup>

<sup>1</sup>Institute of Nature and Environmental Technology, Kanazawa University, Kanazawa, 920-1156, Japan

<sup>2</sup>Institute of Environmental Radioactivity, Fukushima University, Fukushima, 960-1296, Japan

<sup>3</sup>Institute of Radiation Emergency Medicine, Hirosaki University, Hirosaki, 036-8564, Japan

**Correspondence:** Yayoi Inomata (yinomata@se.kanazawa-u.ac.jp)

Received: 27 October 2017 – Discussion started: 29 November 2017

Revised: 19 July 2018 – Accepted: 3 August 2018 – Published: 24 August 2018

**Abstract.** This study investigated the spatio-temporal variations in activity concentrations in the Sea of Japan (SOJ) of  $^{137}\text{Cs}$  and these transport process from the North Pacific Ocean to the SOJ through the East China Sea (ECS) during 2012–2016. The  $^{137}\text{Cs}$  activity concentrations in the SOJ have been increasing since 2012–2013 and reached a maximum in 2015–2016 of approximately  $3.4\text{ Bq m}^{-3}$ , more than twice the pre-Fukushima accident  $^{137}\text{Cs}$  activity concentration of  $\sim 1.5\text{ Bq m}^{-3}$ . The  $^{134}\text{Cs}/^{137}\text{Cs}$  activity ratios ranged from 0.36 to 0.51 in 2016. After taking into account radioactive decay and ocean mixing, we concluded that these  $^{134}\text{Cs}/^{137}\text{Cs}$  activity ratios were evidence that the Fukushima accident caused the increase in the  $^{137}\text{Cs}$  activity concentrations. In the North Pacific south of Japan (NPSJ), the highest  $^{137}\text{Cs}$  activities in 2012–2013 were observed in water from a depth of 300 m, the potential water density anomaly ( $\sigma_\theta$ ) of which corresponded to subtropical mode water (STMW). In the ECS, a clear increase in the  $^{137}\text{Cs}$  activity concentration started at a depth of 140 m ( $\sigma_\theta = 25.2\text{ kg m}^{-3}$ ) in April 2013, propagated to the surface layers at depths of roughly 0–50 m, reached a maximum in 2015 and decreased in subsequent years. In the ECS, the Fukushima-derived radiocaesium activity concentration in surface water reached a maximum in 2014–2015, whereas the concentration in the SOJ reached a maximum in 2015–2016. The propagation of Fukushima-derived radiocaesium in surface seawater from the ECS into the SOJ therefore required approximately 1 year. These temporal changes in  $^{137}\text{Cs}$  activity concentrations and  $^{134}\text{Cs}/^{137}\text{Cs}$  activity ratios indicated that part of the  $^{137}\text{Cs}$  and  $^{134}\text{Cs}$  derived from the Fukushima accident (FNPP1-derived  $^{137}\text{Cs}$  and  $^{134}\text{Cs}$ ) was

transported within several years to the ECS and then to the SOJ via STMW from the NPSJ. The integrated amount of FNPP1-derived  $^{137}\text{Cs}$  that entered the SOJ before 2016 was estimated to be  $0.21 \pm 0.01\text{ PBq}$ , 5.0 % of the estimated total amount of FNPP1-derived  $^{137}\text{Cs}$  in the STMW. The integrated amount of FNPP1-derived  $^{137}\text{Cs}$  that returned to the North Pacific Ocean through the Tsugaru Strait was estimated to be  $0.09 \pm 0.01\text{ Bq}$ , 43 % of the total amount of FNPP1-derived  $^{137}\text{Cs}$  transported to the SOJ and 2.1 % of the estimated total amount of FNPP1-derived  $^{137}\text{Cs}$  in the STMW.

## 1 Introduction

The Fukushima Dai-ichi Nuclear Power Plant (FNPP1) accident in March 2011 released radiocaesium ( $^{137}\text{Cs}$ , half-life 30.2 years, and  $^{134}\text{Cs}$ , half-life 2.06 years) directly into the air and also directly discharged contaminated water to the ocean, primarily in March and April 2011. Eighty per cent of the radiocaesium released to the atmosphere was deposited on the surface of the ocean (Aoyama et al., 2016a; Buesseler et al., 2016; Hirose, 2016; Tsumune et al., 2013). The  $^{137}\text{Cs}$  activity concentration in the surface seawater of the North Pacific Ocean after the FNPP1 accident ranged from a few  $\text{Bq m}^{-3}$  to about  $1\text{ kBq m}^{-3}$  (e.g. Aoyama et al., 2013a, b; Honda et al., 2012; Kaeriyama et al., 2013, 2014). A basin-scale assessment indicated that the FNPP1-derived radiocaesium was confined to a region from 25 to 50° N and from 135° E to 135° W in April and May 2011 (e.g. Aoyama et al., 2013b, 2016a; Inomata et al., 2016; Tsubono et al., 2016).

At latitudes as far north as  $\sim 40^\circ$  N, the radiocaesium was transported eastwards at a rate of approximately  $8 \text{ cm s}^{-1}$  by North Pacific currents such as the Kuroshio and Kuroshio Extension. It reached  $165^\circ$  E in July–September 2011 and the 180th meridian in January–March 2012 (Aoyama et al., 2013b). FNPP1-derived radiocaesium was also found further south in the North Pacific Ocean, where there was a subsurface maximum of  $^{137}\text{Cs}$  at a depth of  $\sim 300 \text{ m}$  (Kaeriyama et al., 2013, 2014, 2016; Kumamoto et al., 2013, 2017). Similar subsurface maxima of  $^{137}\text{Cs}$  were found in subtropical mode water (STMW; potential water density anomaly ( $\sigma_\theta$ )  $25.0\text{--}25.6 \text{ kg m}^{-3}$ ; Masuzawa, 1969) and central mode water (CMW;  $\sigma_\theta = 26.0\text{--}26.5 \text{ kg m}^{-3}$ ) (Aoyama et al., 2016a; Kumamoto et al., 2014, 2015). Aeolian  $^{137}\text{Cs}$  deposited south of the Kuroshio Extension was apparently subducted into the STMW and transported southwards within 10 months after the FNPP1 accident. Rossi et al. (2013) have reported that simulated FNPP1-derived  $^{137}\text{Cs}$  penetrated into the ocean interior via intense subduction and vertical mixing during the winter in the region of mode water formation as described by Oka and Qiu (2012). Kamidaira et al. (2018) have also reported that their model simulation reproduced relatively high  $^{137}\text{Cs}$  activity concentration below the mixed layer. Their simulation indicated that about 43 % of FNPP1-derived  $^{137}\text{Cs}$  was transported below the mixed layer by eddy processes.

Before the FNPP1 accident,  $^{137}\text{Cs}$  was injected into the environment as a result of the large-scale atmospheric nuclear weapons tests that occurred in the late 1950s and early 1960s and the Chernobyl accident in 1986. Caesium-137 was therefore present in the North Pacific Ocean and its marginal seas (Aoyama et al., 2006; Aoyama, 2010; Inomata et al., 2009, 2012). Russia and the former USSR dumped radioactive waste into the northern part of the Sea of Japan (SOJ), although this dumping caused no significant increase in the activity concentrations of  $^{137}\text{Cs}$  (Miyao et al., 1998). During the 2000s, the distribution of  $^{137}\text{Cs}$  activity concentrations was almost homogeneous in the Pacific Ocean, although the activities were relatively high in the western part of the subtropical gyre in the North Pacific Ocean ( $>2 \text{ Bq m}^{-3}$ ) and the South Pacific Ocean ( $>1.5 \text{ Bq m}^{-3}$ ) (Aoyama et al., 2013a). There have hence been two sources of  $^{137}\text{Cs}$  in the North Pacific Ocean and its marginal seas: the  $^{137}\text{Cs}$  released by global fallout (global fallout-derived  $^{137}\text{Cs}$ ) and FNPP1-derived  $^{137}\text{Cs}$ . In contrast, the  $^{134}\text{Cs}$  derived from global fallout and the Chernobyl accident had decayed to below the limit of detection by 1993 because of its 2-year half-life (Miyao et al., 1998). Therefore,  $^{134}\text{Cs}$  has been a satisfactory chemical tracer of the radiocaesium derived from the FNPP1 accident.

Atmospheric deposition of radiocaesium after the FNPP1 accident caused activity concentrations of radiocaesium in the north-eastern SOJ in May 2011 ( $1.5\text{--}2.8 \text{ Bq m}^{-3}$ ) to be approximately 1–2 times the activity concentrations before the FNPP1 accident ( $\sim 1.5 \text{ Bq m}^{-3}$ ) (Fig. 1). By the end of

2011, the  $^{137}\text{Cs}$  activity concentrations in the north-eastern part of the SOJ had decreased rapidly to almost the same levels as before the FNPP1 accident (Inoue et al., 2012).

The SOJ, the main region of interest in this study, is located between the Eurasia and the Japanese archipelago. It has an area of  $1.013 \times 10^6 \text{ km}^2$  and a mean depth of  $1.67 \text{ km}$  (Menard and Smith, 1966). The south-western SOJ is connected to the East China Sea (ECS) through Tsushima-kaikyō, and the north-eastern SOJ is connected to the North Pacific Ocean through the Tsugaru Strait. Warm, saline seawater passes through Tsushima-kaikyō via the Tsushima Warm Current (TWC). This current splits into two separate currents. One is the nearshore current that flows along the west coast of Honshū Island, Japan. Some of this water passes through the Tsugaru Strait and into the Pacific Ocean. The remainder is transported to the north and passes through Sōya-kaikyō into the Sea of Okhotsk. The other current flows north of the Korean Peninsula. This current meets the North Korean Cold Current, which is an extension of the Liman Cold Current. This northward-flowing warm, subtropical water meets southward-flowing cold, subarctic SOJ waters to form the polar front at approximately  $40^\circ$  N. The SOJ is therefore divided largely into two regions (Prants et al., 2015). The current system in and around the SOJ should be taken into consideration when assessing the spatio-temporal variations in radiocaesium derived from global fallout and the FNPP1 accident.

The purposes of this study were to (1) investigate the spatio-temporal variations in activity concentrations in the SOJ of  $^{137}\text{Cs}$  released as a result of the FNPP1 accident, (2) investigate the processes responsible for transport of radiocaesium from the North Pacific Ocean to the SOJ through the East China Sea, and (3) estimate the amount of FNPP1-derived  $^{137}\text{Cs}$  transported into the SOJ through Tsushima-kaikyō as well as the amount of FNPP1-derived  $^{137}\text{Cs}$  returned into the North Pacific Ocean through the Tsugaru Strait during 2012–2016 and the uncertainties of these estimates.

## 2 Sampling, measurements and methods

### 2.1 Data sources

After the FNPP1 accident, many radiocaesium measurements were taken in the SOJ and western North Pacific Ocean (Fig. 1). To elucidate the temporal and spatial distributions of the radiocaesium activity concentrations, we used as many data points as possible. We therefore compiled all available data from the literature and reported studies. Most of the data before the FNPP1 accident are included in the database “Historical Artificial Radionuclides in the Pacific Ocean and its Marginal Seas” (HAM database) (Aoyama and Hirose, 2004, and their updated version). The data recorded after the FNPP1 accident have been presented by Aoyama et

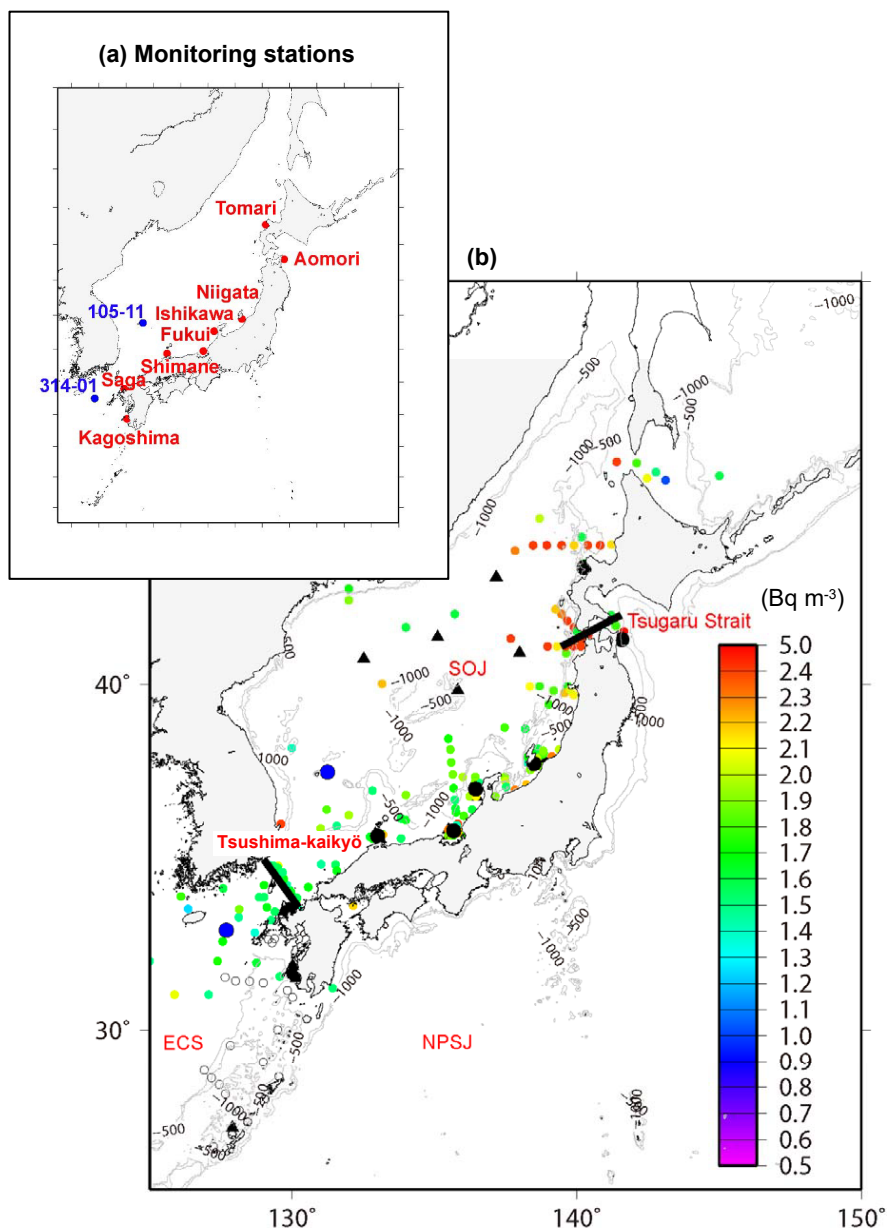


**Figure 1.** Location of the sampling points after the FNPP1 accident. Large black circles are sites monitored by the Japanese government. Blue circles are sites monitored by the Korean government. Black triangles are sites with measured vertical profiles. The colours of other circles correspond to the  $^{137}\text{Cs}$  activity concentrations measured in 2011. Open circles are sites measured after 2012. The area around Japan was divided into three regions: the SOJ, ECS and NPSJ ( $< 141.5^\circ\text{E}$ ). The locations of monitoring stations are also plotted in (a).

al. (2016a). The term “surface seawater” as used in this study refers to a sample collected at a depth of less than 10 m.

We also focused on the Japanese government’s monitoring data collected at Tomari ( $42.98\text{--}43.17^\circ\text{N}$ ,  $140.21\text{--}140.30^\circ\text{E}$ ), Aomori ( $41.13\text{--}41.22^\circ\text{N}$ ,  $141.50\text{--}141.67^\circ\text{E}$ ), Niigata ( $37.62\text{--}38.10^\circ\text{N}$ ,  $138.38\text{--}138.84^\circ\text{E}$ ), Ishikawa ( $36.87\text{--}37.29^\circ\text{N}$ ,  $136.43\text{--}136.47^\circ\text{E}$ ), Fukui ( $35.75\text{--}36.09^\circ\text{N}$ ,  $135.50\text{--}135.83^\circ\text{E}$ ), Shimane ( $35.67\text{--}35.80^\circ\text{N}$ ,  $132.87\text{--}133.2^\circ\text{E}$ ), Saga ( $33.57\text{--}33.62^\circ\text{N}$ ,

$129.73\text{--}129.98^\circ\text{E}$ ) and Kagoshima ( $31.58\text{--}31.93^\circ\text{N}$ ,  $130.02\text{--}130.15^\circ\text{E}$ ) (Marine Ecology Research Institute, 2011, 2012, 2013, 2014, 2015, 2016) (Fig. 1). These measurements, except for the Aomori sites, were taken once a year (from the middle of May to early June). Near the Aomori sites, offshore monitoring was also conducted twice a year (May and October) at the Rokkasho Reprocessing Plant ( $39.5\text{--}41.4^\circ\text{N}$ ,  $141.5\text{--}142.3^\circ\text{E}$ ). Seawater was sampled at various depths, from the surface to 664 m, at each

monitoring site. Monitoring data (site 304-01: 33.0° N, 127.7° E; site 105-11: 37.3° N, 131.3° E) from the Korean government were also used in this analysis (Korea Institute of Nuclear Safety, 2011, 2012, 2013, 2014, 2015, 2016) (Fig. 1). At these monitoring sites, surface seawater (0 m depth) measurements were taken four times (February, April, August and October) each year.

## 2.2 Measurement of $^{134}\text{Cs}$ activity concentrations

The  $^{134}\text{Cs}$  activity concentrations in most of the monitoring datasets were below the limit of detection because of the low sensitivity of the measurement methods. We also collected seawater samples to investigate the spatial distribution of  $^{134}\text{Cs}$  activity concentrations. The sample volumes ranged from a few litres to 10 L. The radiocaesium in the sampled seawater was extracted using the ammonium phosphomolybdate (AMP)–Cs compound method as improved by Aoyama and Hirose (2008). The  $^{134}\text{Cs}$  and  $^{137}\text{Cs}$  activity concentrations in the AMP–Cs compound were determined with the ultra-low-background gamma-ray detectors in the Low Level Radioactivity Concentration Laboratory of Kanazawa University (Hamajima and Komura, 2004). Aoyama and Hirose (2008) and Aoyama et al. (2016a) have described the measurement procedure in detail. All radioactivity concentrations shown in this research were decay-corrected to the time of sample collection. In addition, we also determined  $^{134}\text{Cs} / ^{137}\text{Cs}$  activity ratios decay-corrected to 11 March 2011, the time of the FNPP1 accident.

## 2.3 Estimation of FNPP1-derived $^{137}\text{Cs}$ activity concentrations

In this study, we estimated the increase in  $^{137}\text{Cs}$  activity concentrations due to the FNPP1 accident. The  $^{137}\text{Cs}$  activity concentrations in the SOJ decreased exponentially after 1965. The decrease in the  $^{137}\text{Cs}$  activity concentrations slowed down from 2000 to 2010 (Fig. 2). By assuming that the apparent half-residence time of global fallout-derived  $^{137}\text{Cs}$  was approximately the same before and after the FNPP1 by using the negative exponential fitted curve, we estimated the global fallout-derived  $^{137}\text{Cs}$  activity concentrations after the accident (Fig. S1 in the Supplement). The FNPP1-derived  $^{137}\text{Cs}$  was then estimated from the difference between the measured activity concentrations and the values extrapolated from the exponential fitted curve during the period 2000–2010 (Fig. S1).

## 2.4 Estimation of amounts of $^{137}\text{Cs}$ transported during 2012–2016

We estimated the amounts of FNPP1-derived  $^{137}\text{Cs}$  transported in each region during 2012–2016 with Eq. (1):

$$\text{Transport amount} = \sum_{i=2012}^n (\text{FNPP1-derived } ^{137}\text{Cs activity concentration in year } i) \times (\text{annual average seawater transport volume in year } i), \quad (1)$$

where  $n = 2016$ . We used the annual average FNPP1-derived  $^{137}\text{Cs}$  activity concentrations at stations Saga and 304-11 for the ECS, station Shimane for the eastern TWC and station 105-01 for the western TWC. We used station Aomori to estimate the amount of FNPP1-derived  $^{137}\text{Cs}$  transported to the North Pacific Ocean via the Tsugaru Strait. The amount of FNPP1-derived  $^{137}\text{Cs}$  transported northwards along the western coast of Hokkaidō was estimated from the difference between the total inflow of FNPP1-derived  $^{137}\text{Cs}$  at the entrance of the Tsugaru Strait its outflow from the strait. The annual average volume of seawater transported through the TWC was estimated from the data of Fukudome et al. (2010) and Han et al. (2016). The average volumes of TWC transported into the SOJ annually ranged from  $2.59 \pm 0.50 \times 10^6$  to  $2.82 \pm 0.58 \times 10^6 \text{ m}^3 \text{ s}^{-1}$ , of which the average volumes of seawater transported through the east and west channels of Tsushima-kaikyō annually were, respectively,  $1.08 \pm 0.26$ – $1.26 \pm 0.27 \times 10^6 \text{ m}^3 \text{ s}^{-1}$  and  $1.43 \pm 0.38$ – $1.56 \pm 0.47 \times 10^6 \text{ m}^3 \text{ s}^{-1}$  during 2012–2016. Nishida et al. (2003) estimated the volume transported through the Tsugaru Strait to be  $1.0$ – $1.3 \times 10^6 \text{ m}^3 \text{ s}^{-1}$ ; we used this value because we did not have in situ monitoring data for this value. The evaluation of seasonal variations was difficult in this study because the monitoring data were limited; relevant fluxes were measured once a year at the Japanese monitoring site and four times a year at the Korean monitoring sites.

## 3 Results

### 3.1 Increased $^{137}\text{Cs}$ activity concentrations in the ECS and the SOJ

Figure 2 shows the temporal variation in the  $^{137}\text{Cs}$  activity concentrations in the surface seawater of the SOJ after the 1960s as well as the half-year average values. The  $^{137}\text{Cs}$  activity concentrations decreased exponentially from 1960 to 1970; these concentrations originated from atmospheric nuclear weapons testing (Aoyama, 2010). The increase in the  $^{137}\text{Cs}$  activity concentrations in 1986 was the result of the Chernobyl accident (Miyao et al., 1998). The apparent half-residence time during the period 1970–1990 was estimated to be  $16.3 \pm 0.5$  years (Inomata et al., 2009). In the 2000s, the magnitude of the rate of decrease in  $^{137}\text{Cs}$  activity concentrations was small, and the half-year average  $^{137}\text{Cs}$  activity

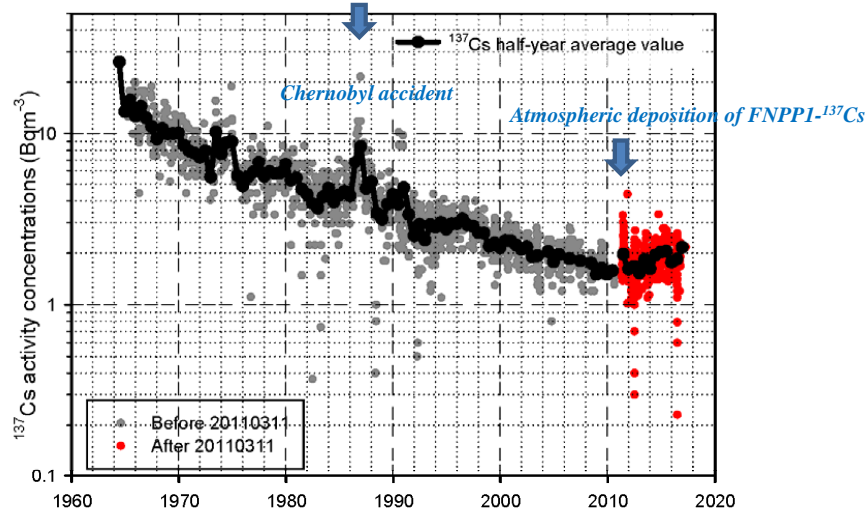


**Figure 2.** Temporal variations in the  $^{137}\text{Cs}$  activity concentrations in surface seawater in the Sea of Japan during the period from 1960 to 2016. Circles indicate measured values, and red circles indicate data measured after the accident (11 March 2011). Black circles indicate the 0.5-year average value. Standard deviations of data were removed to clearly show the temporal variation.

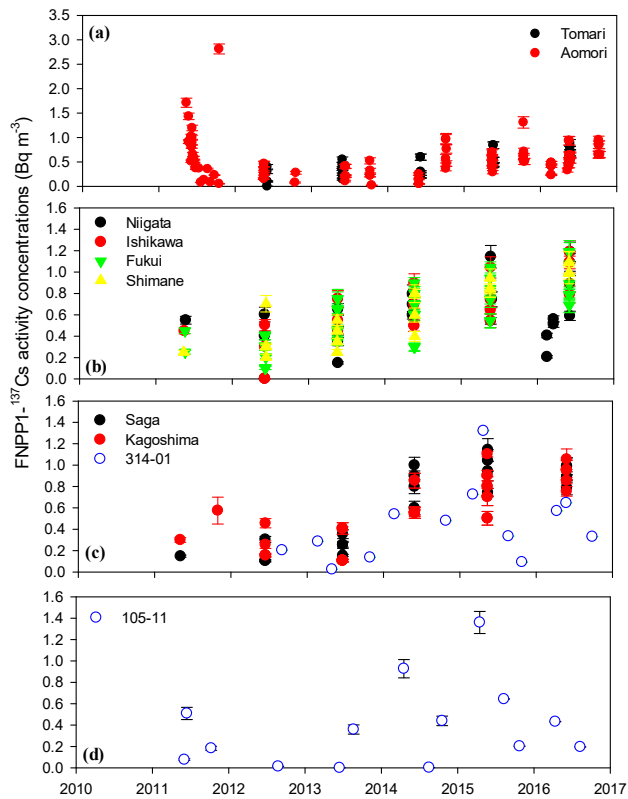
concentrations in the surface seawater reached a low of 1.5–2.4  $\text{Bq m}^{-3}$ . Within several months after the FNPP1 accident, high activity concentrations of  $^{137}\text{Cs}$ , up to 3.3  $\text{Bq m}^{-3}$ , were observed. The  $^{137}\text{Cs}$  activity concentrations were higher in the north-eastern part of the SOJ than in the south-western part of the SOJ (Fig. 1). These high  $^{137}\text{Cs}$  activity concentrations were associated with wet deposition of  $^{137}\text{Cs}$  released into the atmosphere during the FNPP1 accident in March–April 2011. In addition to the abrupt increase in the  $^{137}\text{Cs}$  activity concentrations just after the FNPP1 accident in 2011, the  $^{137}\text{Cs}$  activity concentrations subsequently increased gradually in the SOJ (Aoyama et al., 2017). The  $^{137}\text{Cs}$  activity concentrations in 2016 reached 2.6  $\text{Bq m}^{-3}$ , which was the same as the concentrations in 1998.

Figure 3 shows the FNPP1-derived  $^{137}\text{Cs}$  activity concentrations measured at monitoring stations in the ECS and SOJ by the Japanese and Korean governments. These monitoring stations are located along a branch of the Kuroshio in the ECS and along the western and eastern TWC in the SOJ. The long-term variations in the  $^{137}\text{Cs}$  activity concentrations and FNPP1-derived  $^{137}\text{Cs}$  at each monitoring station are also shown in Figs. S2–9. With the exception of the high activity concentrations at Aomori in 2011, caused by the wet deposition of FNPP1-derived  $^{137}\text{Cs}$  released to the atmosphere, an increase in the FNPP1-derived  $^{137}\text{Cs}$  in the SOJ started in 2012 and 2013. The FNPP1-derived  $^{137}\text{Cs}$  gradually increased up to 1.3  $\text{Bq m}^{-3}$  in 2016 (Fig. 3a, b). The lower activity concentrations at Niigata (Fig. 3b) were because the measurements were made at a station near Sado Island, off Niigata, rather than at the usual government monitoring site. At these monitoring stations, there was no significant trend of decreasing FNPP1-derived  $^{137}\text{Cs}$  activity concentrations

in 2015 and 2016. In contrast, the FNPP1-derived  $^{137}\text{Cs}$  activity concentrations at stations upstream from the SOJ in the ECS (Fig. 3c; Kagoshima, Saga and station 314-01) increased beginning in 2012–2013. The increase was clearly apparent after 2014 in the ECS. The FNPP1-derived  $^{137}\text{Cs}$  activity concentrations were slightly lower in 2016 than in 2015. At station 105-11, which was located off South Korea (Fig. 1), marked increases in FNPP1-derived  $^{137}\text{Cs}$  activity concentrations were observed in 2014, and FNPP1-derived  $^{137}\text{Cs}$  activity concentrations reached approximately 1.4  $\text{Bq m}^{-3}$  in 2015 (Fig. 3d). The FNPP1-derived  $^{137}\text{Cs}$  concentrations were lower in 2016 than in preceding years.

The  $^{134}\text{Cs}/^{137}\text{Cs}$  activity ratios in 2016 ranged from 0.27 to 0.51 (Fig. 4). There was no significant difference in the  $^{134}\text{Cs}/^{137}\text{Cs}$  activity ratios among the stations in the ECS and the SOJ.

Figure 5 shows the temporal variations in the  $^{137}\text{Cs}$  activity concentrations at different depths at station 314-01 in the ECS (Fig. 5a; 0–140 m) and at station 105-11 in the SOJ (Fig. 5b; 0–2000 m). Increases in the  $^{137}\text{Cs}$  activity concentrations in the subsurface layer (at 140 m and 200 m at stations 314-01 and 105-11, respectively) occurred in 2013, approximately 1 year earlier than in the shallower layers. At station 314-01, the  $^{137}\text{Cs}$  activity concentrations at a depth of 140 m were higher than those at the surface beginning in 2013. They increased up to  $3.2 \pm 0.28 \text{ Bq m}^{-3}$  in 2014 and then tended to decrease after 2015. At shallower depths (0–50 m),  $^{137}\text{Cs}$  activity concentrations increased in 2014 and did not significantly decrease in 2015 and 2016. At station 105-11, the increase in the  $^{137}\text{Cs}$  activity concentrations started earlier in the subsurface seawater (200 m depth) in 2013. In 2014, the  $^{137}\text{Cs}$  activity concentrations in surface



**Figure 3.** Temporal variations in the FNPP1-derived  $^{137}\text{Cs}$  activity concentrations in the surface seawater at the monitoring sites in Japan after 2011. FNPP1-derived  $^{137}\text{Cs}$ : (a) Tomari, Aomori, (b) Niigata, Ishikawa, Fukui, Shimane, (c) Saga, Kagoshima, 314-01 and (d) 105-11.

seawater also increased and reached  $2.8 \pm 0.2 \text{ Bq m}^{-3}$  in 2015. Decreases in the  $^{137}\text{Cs}$  activity concentrations at 200 m and at the surface were observed after 2015, and a subsurface peak in the  $^{137}\text{Cs}$  activity concentration at 200 m was not observed after 2015. Similar variations characterised by an increase in the  $^{137}\text{Cs}$  activity concentration that started from the ocean interior were observed at the Kagoshima and Saga monitoring stations (Fig. S10).

### 3.2 Propagation of radiocaesium from the upstream region (NPSJ and ECS) to the downstream region (the SOJ)

Figure 6 shows the distributions of the  $^{137}\text{Cs}$  activity concentrations versus depth and  $\sigma_\theta$  in the North Pacific South of Japan (NPSJ), in the ECS and at station 105-11. In the NPSJ, the  $^{137}\text{Cs}$  activity concentrations reached subsurface maxima of  $8.2\text{--}12.3 \text{ Bq m}^{-3}$  at approximately 300 m depth in 2012–2013 (Fig. 6a). Those high  $^{137}\text{Cs}$  activity concentrations were measured in the region bounded by  $136\text{--}138^\circ \text{ E}$  and  $26\text{--}30^\circ \text{ N}$ . After 2014, a subsurface peak in the  $^{137}\text{Cs}$  activity concentration was not observed. The location of these

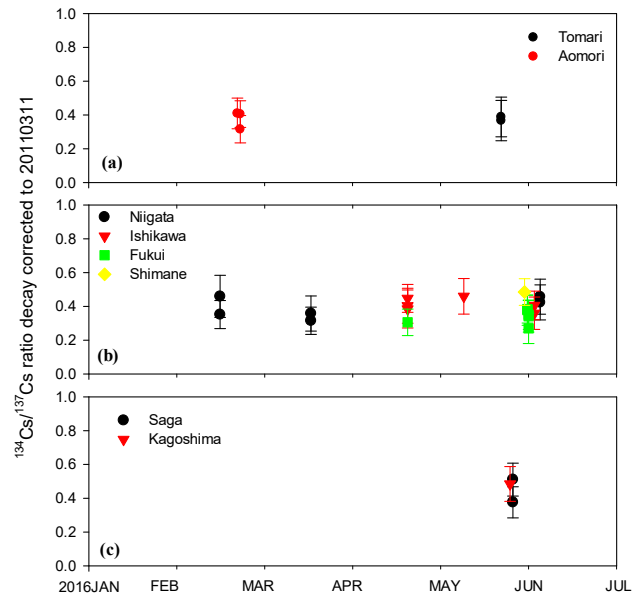


**Figure 4.** Temporal variations in the  $^{134}\text{Cs}/^{137}\text{Cs}$  activity concentration ratio in the surface seawater at the monitoring stations in Japan from January 2016 to June 2016. (a) Tomari, Aomori, (b) Niigata, Ishikawa, Fukui, Shimane, (c) Saga and Kagoshima.

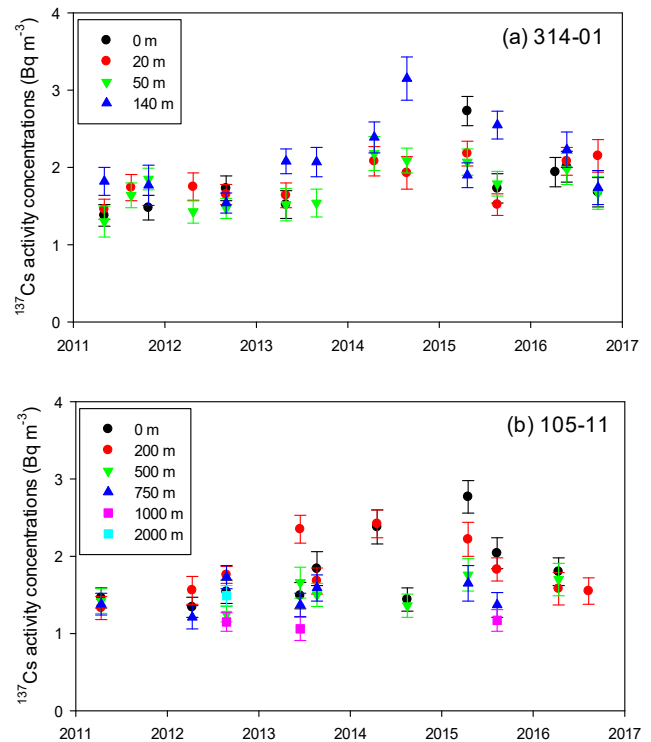


**Figure 5.** Temporal variations in the  $^{137}\text{Cs}$  activity concentrations at stations (a) 314-01 and (b) 105-11.

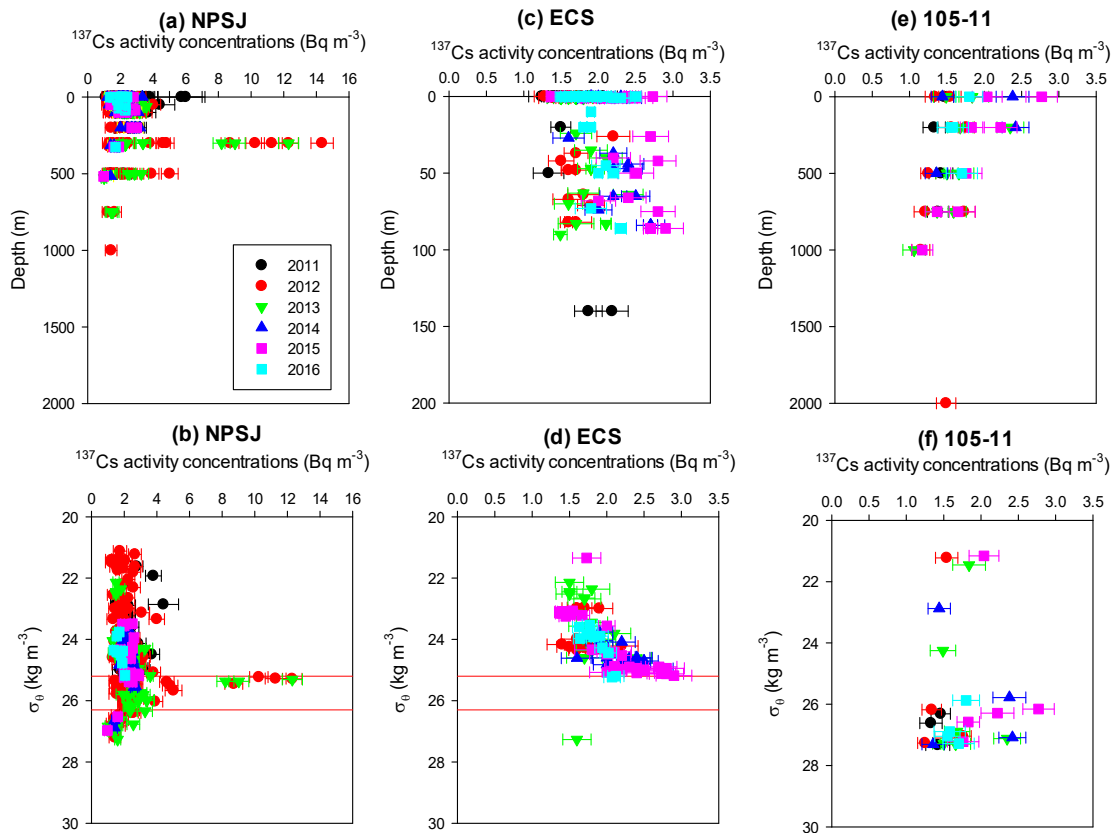


**Figure 6.** Vertical distributions of the  $^{137}\text{Cs}$  activity concentrations over the (a) depth profile in the NPSJ, (b) potential water density anomaly profile in the NPSJ, (c) depth profile in the ECS, (d) potential water density profile in the ECS, (e) depth profile at 105-01 along the WTWC and (f) potential water density anomaly profile at 105-01 along the western TWC. Colour indicates the collection time (year).

subsurface peaks in  $^{137}\text{Cs}$  activity concentrations in the layer corresponding to a  $\sigma_\theta$  of  $25.2\text{ kg m}^{-3}$  (Fig. 6b) is consistent with previous findings of a  $^{137}\text{Cs}$  activity maximum in STMW with a  $\sigma_\theta$  of  $25.0\text{--}25.6\text{ kg m}^{-3}$  (Kaeriyama et al., 2014; Kumamoto et al., 2014). In the ECS, the  $^{137}\text{Cs}$  activity concentrations gradually increased beginning in 2012 and reached a maximum ( $2.9 \pm 0.24\text{ Bq m}^{-3}$ ) in 2015. The concentrations decreased in 2016 (Fig. 6c). High  $^{137}\text{Cs}$  activity concentrations ( $>2\text{ Bq m}^{-3}$ ) in the ECS were found in the layer corresponding to  $\sigma_\theta$  values of  $23.6\text{--}25.2\text{ kg m}^{-3}$  (Fig. 6d). In contrast,  $^{137}\text{Cs}$  activity concentrations at station 105-11 in the western SOJ decreased with increasing depth until 500 m (Fig. 6e). The highest  $^{137}\text{Cs}$  activity concentrations that exceeded  $2\text{ Bq m}^{-3}$  at station 105-11, except in one sample measured in 2015, were found at  $\sigma_\theta$  values of  $25.8\text{--}27.1\text{ kg m}^{-3}$  (Fig. 6f).

Figure 7 shows Hovmöller diagrams of  $^{137}\text{Cs}$  activity concentrations at  $\sigma_\theta$  values of  $25.2 \pm 0.5\text{ kg m}^{-3}$  along the TWC in the ECS and at coastal sites in the eastern SOJ. These  $\sigma_\theta$  surfaces were selected to show the maximum  $^{137}\text{Cs}$  activity

concentrations in the ECS. Figure S11 shows the vertical distributions of the  $^{137}\text{Cs}$  activity concentrations with depth and  $\sigma_\theta$  at each monitoring station. Note that in the SOJ, the vertical distributions of the  $^{137}\text{Cs}$  activity concentrations below 250 m were almost constant, and a subsurface peak of  $^{137}\text{Cs}$  was not found at the monitoring stations along the eastern TWC (Fig. S11). The  $^{137}\text{Cs}$  activity concentrations before the FNPP1 accident were approximately  $1.5\text{ Bq m}^{-3}$ . In the ECS, the  $^{137}\text{Cs}$  activity concentrations gradually increased and attained maxima during 2014–2015 (Fig. 7). The  $^{137}\text{Cs}$  activity concentrations in the ECS tended to decrease in 2016 in a layer with a  $\sigma_\theta$  of  $25.2 \pm 0.5\text{ kg m}^{-3}$ . In the south-western part of the SOJ (Shimane, Fukui, Ishikawa and Niigata), the  $^{137}\text{Cs}$  activity concentrations gradually increased beginning in 2012 and reached a maximum of  $2.5\text{ Bq m}^{-3}$  during 2015–2016; those trends were almost the same as the trends at the monitoring stations in the ECS. In the north-western SOJ (Aomori and Tomari), the  $^{137}\text{Cs}$  activity concentrations increased slightly and exceeded  $2\text{ Bq m}^{-3}$  in 2016. These results indicate that the propagation of FNPP1-derived  $^{137}\text{Cs}$  from the ECS ( $32\text{--}34^\circ\text{ N}$ ) to the SOJ ( $35\text{--}38^\circ\text{ N}$ ) along the TWC (Fig. 7) occurred within 1 year.

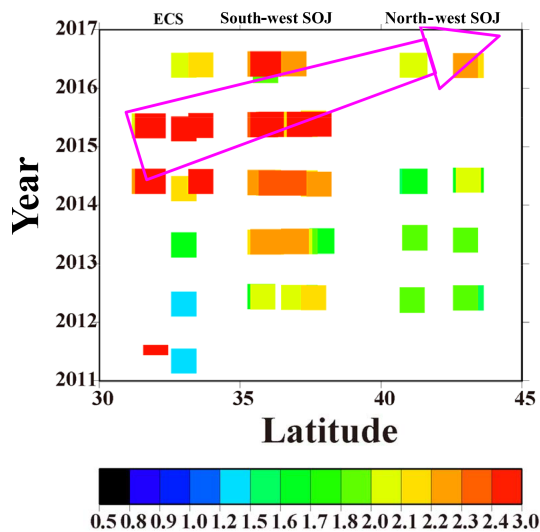


**Figure 7.** Hovmöller diagrams of the  $^{137}\text{Cs}$  activity concentrations at a potential water density anomaly of  $25.2 \pm 0.5 \text{ kg m}^{-3}$  along with an eastern TWC. The ECS stations described on the  $x$  axis are Kagoshima and Saga stations. The south-western SOJ includes the monitoring stations Shimane, Fukui, Ishikawa and Niigata. The north-western SOJ includes the monitoring stations Aomori and Tomari. Colour indicates the  $^{137}\text{Cs}$  activity concentrations ( $\text{Bq m}^{-3}$ ).

### 3.3 Transport process and total amount of FNPP1-derived $^{137}\text{Cs}$ transported into the SOJ during 2012–2016

Here we describe the possible pathway of FNPP1-derived  $^{137}\text{Cs}$  from the Pacific Ocean to the SOJ via the ECS. The westward-flowing undercurrent would have transported FNPP1-derived  $^{137}\text{Cs}$  in the STMW south-westwards, as reported by Oka (2009). The  $^{137}\text{Cs}$  entrained in the STMW would have reached the western boundary of the SOJ at lower latitudes and become entrained into the Kuroshio (Oka and Qiu, 2012) before being transported northwards to the west of Kyushu by the TWC bifurcation from the Kuroshio. The FNPP1-derived  $^{137}\text{Cs}$  would then have entered the SOJ through Tsushima-kaikyō via the TWC. FNPP1-derived  $^{137}\text{Cs}$  transported by the TWC would have been divided into western (coastal stations in Korea) and eastern (eastern coast of the Japanese Islands) portions. The remaining FNPP1-derived  $^{137}\text{Cs}$  in the eastern TWC would have been transported northwards along the western coast of Hokkaidō (Fig. 8). The integrated FNPP1-derived  $^{137}\text{Cs}$  in the ECS during 2012–2016 was estimated to be  $0.21 \pm 0.01 \text{ PBq}$ , which corresponds to 5.0 % of the FNPP1-derived  $^{137}\text{Cs}$  in the STMW ( $4.2 \pm 1.1 \text{ PBq}$ ) estimated by Kaeriyama et al. (2016) (Table 1). The bifurcation of the TWC resulted in transport of  $0.11 \pm 0.01 \text{ PBq}$  of FNPP1-derived  $^{137}\text{Cs}$  in the eastern channel, which corresponds to 2.6 % of the FNPP1-derived  $^{137}\text{Cs}$  in the STMW. The amount of FNPP1-derived

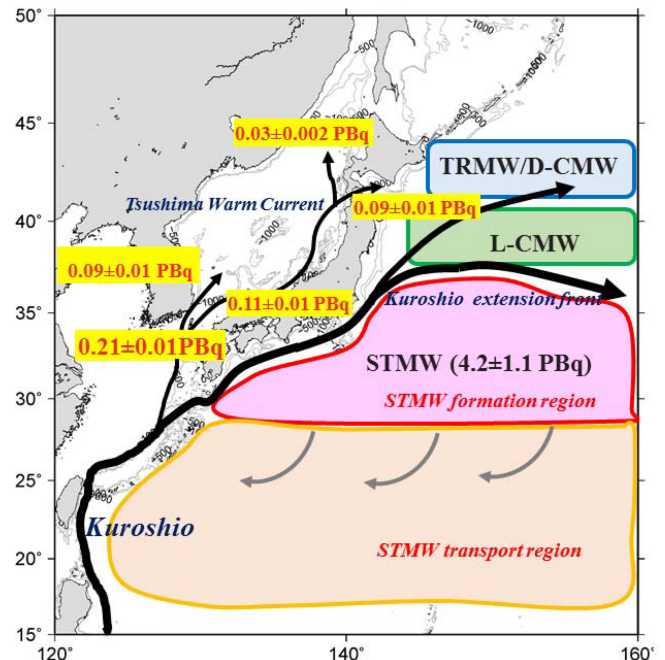


**Figure 8.** Schematic diagram of the FNPP1-derived  $^{137}\text{Cs}$  transport in the North Pacific Ocean. The bold line indicates the Kuroshio pathway. The thin black lines indicate the flow pathway of the Tsushima Warm Current. The pink region is the STMW formation area. The green region is the lighter variety of the CMW (L-CMW) formation area, and the blue region indicates the Transition Region Mode Water (TRMW) and the denser variety of the CMW (D-CMW) formation area. The estimated accumulated flux during the period from 2012 to 2016 at each section is shown. The inventory in the STMW was deduced by Kaeriyama et al. (2016).

$^{137}\text{Cs}$  transported in the western channel was estimated to be  $0.09 \pm 0.01 \text{ PBq}$ , which corresponds to 2.1 % of the FNPP1-derived  $^{137}\text{Cs}$  injected into the STMW. The amounts of FNPP1-derived  $^{137}\text{Cs}$  in the eastern and western outflows are consistent with the range of uncertainty for the inflow amounts:  $0.21 \pm 0.01 \text{ PBq}$ . A small part of the transported FNPP1-derived  $^{137}\text{Cs}$  ( $0.09 \pm 0.01 \text{ PBq}$ ; 2.1 % of FNPP1-derived  $^{137}\text{Cs}$  in STMW) was returned to the North Pacific Ocean via transport through the Tsugaru Strait. In other words, the amount of FNPP1-derived  $^{137}\text{Cs}$  that was returned to the North Pacific Ocean corresponded to 43 % of the total amount of FNPP1-derived  $^{137}\text{Cs}$  transported to the SOJ and 2.1 % of the estimated total amount of FNPP1-derived  $^{137}\text{Cs}$  in the STMW. The remaining  $0.03 \pm 0.002 \text{ PBq}$  (14 % of the transported FNPP1-derived  $^{137}\text{Cs}$  in the SOJ; 0.7 % of the transported FNPP1-derived  $^{137}\text{Cs}$  in STMW) would have been transported to the northern part of the SOJ (west of Hokkaidō) or, in part, to the interior of the ocean via deep convection and surface mixing.

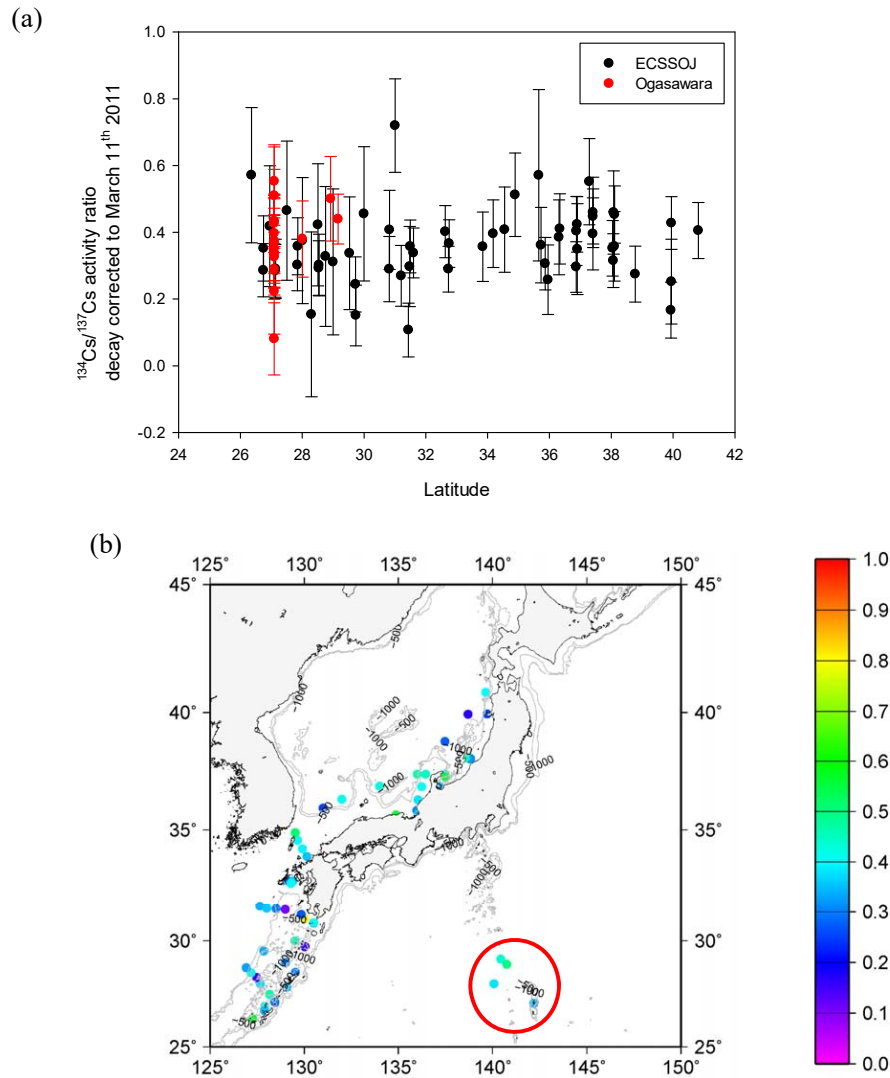


**Figure 9.** Latitudinal and horizontal distributions of the  $^{134}\text{Cs}/^{137}\text{Cs}$  activity ratios measured at the coastal sites of the SOJ and ECS in 2015–2016. The values were radioactive decay-corrected to 11 March 2011. The data measured in the Ogasawara area (red circle in **b**) were also added. **(a)** Latitudinal distribution; **(b)** horizontal distribution.

## 4 Discussion

### 4.1 Signature of FNPP1-derived $^{137}\text{Cs}$ inflow in the SOJ by using the $^{134}\text{Cs}/^{137}\text{Cs}$ activity ratio

According to atmospheric model simulations, atmospheric deposition of FNPP1-derived  $^{137}\text{Cs}$  occurred over a wide region in the western North Pacific Ocean (30–55° N, 140–180° E) (e.g. Aoyama et al., 2016b). One of the regions where  $^{137}\text{Cs}$  was deposited south of the Kuroshio and Kuroshio Extension corresponded to the region of STMW formation (Aoyama et al., 2016b; Oka et al., 2012). The release of FNPP1-derived radiocaesium into the atmosphere occurred at the end of March and in early April 2011. Because the deposition of FNPP1-derived  $^{137}\text{Cs}$  into the North

Pacific Ocean was therefore a point source with respect to time, FNPP1-derived radiocaesium is a very useful tracer for investigating the transport of FNPP1-derived radiocaesium in the North Pacific Ocean. The vertical distributions of the  $^{137}\text{Cs}$  activity concentrations in the NPSJ indicated that FNPP1-derived  $^{137}\text{Cs}$  was entrained in STMW (Fig. 6).

There were several indicators of the transport process: (i) maximum  $^{137}\text{Cs}$  activity concentrations were observed in the subsurface layer rather than the surface seawater; (ii)  $\sigma_\theta$  data indicated that the  $^{137}\text{Cs}$  activity concentrations were highest in STMW; (iii) in the ECS, the similarity of the  $\sigma_\theta$  of  $^{137}\text{Cs}$ -contaminated seawater to the  $\sigma_\theta$  of STMW is an indication that FNPP1-derived  $^{137}\text{Cs}$  was transported into the ECS via STMW from the NPSJ; and (iv) the  $^{137}\text{Cs}$  activ-

**Table 1.** Estimated transport amount of FNPP1-derived  $^{137}\text{Cs}$  in the monitoring site in the SOJ along with the Tsushima Warm Current.

Flow	Station	Transport amount (PBq)*	Ratio against to STMW (%)	Ratio against to inflow into the SOJ (%)
Inflow to SOJ				
ECS to SOJ	Saga/304-01	$0.21 \pm 0.01$	$5.0 \pm 2.3$	
At Tsushima-kaikyō				
Western TWC	105-11	$0.09 \pm 0.01$	$2.1 \pm 1.2$	$43 \pm 10$
Eastern TWC	Shimane	$0.11 \pm 0.01$	$2.6 \pm 1.4$	$50 \pm 7$
Two branches of eastern TWC				
Outflow to Pacific Ocean	Aomori off	$0.09 \pm 0.01$	$2.1 \pm 1.2$	$43 \pm 10$
Northward transport	Tomari	$0.03 \pm 0.002$	$0.7 \pm 0.3$	$14 \pm 2$

\* The value was decay-corrected to 11 March 2011. ECS were estimated by using the average value of the 314-01 and Saga monitoring sites. The transport amount (\*) was estimated by sum of the duration from 2012 to 2016.

ity concentrations in the northern ECS ( $> 30^\circ \text{N}$ ) were higher than those in the southern ECS ( $< 30^\circ \text{N}$ ) (Fig. S12). In this study, however, there were not enough data to elucidate the transport route in more detail.

Figure 9 shows the latitudinal distribution of the  $^{134}\text{Cs} / ^{137}\text{Cs}$  activity ratio, which was decay-corrected to 11 March 2011. The  $^{134}\text{Cs} / ^{137}\text{Cs}$  activity ratio ranged from 0.1 to 0.72, and the ratios in the Ogasawara region and in the ECS were almost the same as those in the SOJ (Fig. 9a). Considering that the  $^{134}\text{Cs} / ^{137}\text{Cs}$  activity ratio in the radiocaesium that originated from the FNPP1 accident was almost 1 (Buesseler et al., 2011), variations in the ratio indicated that seawater contaminated with FNPP1-derived radiocaesium had mixed with seawater contaminated with global fallout-derived radiocaesium during transport. The highest activity concentration ratio (0.72), which was found near Kagoshima, is an indication of the highest contribution of FNPP1-derived radiocaesium. In contrast, the relatively low  $^{134}\text{Cs} / ^{137}\text{Cs}$  activity ratio in the region bounded by  $30\text{--}32^\circ \text{N}$  implies a small contribution of FNPP1-derived radiocaesium to that region of the Pacific Ocean. Within the ECS, the  $^{137}\text{Cs}$  activity concentrations tended to increase northwards as suggested by Aoyama et al. (2017) (Fig. S12). The  $^{137}\text{Cs}$  activity concentrations measured at Okinawa in the southern ECS (<http://search.kankyo-hoshano.go.jp/servlet/search.top?pageSID=113836570>; last access: 17 August 2018) averaged approximately  $1.7 \pm 0.47 \text{ Bq m}^{-3}$ , slightly higher than those measured before the FNPP1 accident (Fig. S13). The implication is that less FNPP1-derived radiocaesium was transported to the southern ECS than to the northern ECS, as shown in Fig. S12.

#### 4.2 Advection and vertical mixing of FNPP1-derived $^{137}\text{Cs}$ in the SOJ

In this study, we revealed that FNPP1-derived  $^{137}\text{Cs}$  entered the SOJ via the ECS. FNPP1-derived  $^{137}\text{Cs}$  was then transported northward with the TWC. In the SOJ, there was a time lag of approximately 1 year in the propagation of FNPP1-derived radiocaesium (Fig. 7). Based on measurements of phosphate, one of the dominant seawater nutrients, Kodama et al. (2016) have revealed that the phosphate concentrations in surface seawater of the SOJ during winter are positively correlated ( $p < 0.05$ ) with the phosphate concentrations in the saline ECS seawater during the preceding summer, and the surface water of the southern SOJ is almost entirely replaced by ECS seawater during May–October. They have also suggested that the transport of water-soluble constituents from the ECS to the SOJ takes at least  $\sim 0.5$  years. The propagation of FNPP1-derived radiocaesium into the SOJ is consistent with the timescale of propagation of changes of nutrient concentrations from the ECS to the SOJ (Kodama et al., 2016).

The  $^{137}\text{Cs}$  activity concentrations at station 105-11, located along the western side of the TWC in the SOJ, were highest at the surface and gradually decreased with increasing depth (Fig. 6e). This vertical distribution differed from those in the NPSJ (Fig. 6a) and ECS (Fig. 6c). In particular, the subsurface peak observed in the NPSJ and ECS did not appear at station 105-11. At station 105-11, most of the  $^{137}\text{Cs}$  was in seawater with a  $\sigma_\theta$  of  $25.7\text{--}27.3 \text{ kg m}^{-3}$  (Fig. 6f), higher than the  $\sigma_\theta$  in the NPSJ and ECS. A similar vertical distribution was also observed along the western coast of the Japanese Islands on the eastern side of the TWC (Fig. S11). These distributions were due to the cooling of the surface layer after water was transported through Tsushima-kaikyō. Physical processes such as the convergence and subduction of surface water inside eddies are important mechanisms of

the downward transport of radiocaesium (Miyao et al., 1998; Budyansky et al., 2015). There is a possibility that the downward transport of radiocaesium is seasonal. The  $^{137}\text{Cs}$  derived from global fallout should have already penetrated below the surface layer and have accumulated in the deeper layers of the SOJ.

### 4.3 Mass balance of FNPP1-derived $^{137}\text{Cs}$ in the SOJ

The most reliable estimates of the amount of FNPP1-derived  $^{137}\text{Cs}$  deposited in the North Pacific Ocean via atmospheric release and direct release to the Ocean are 11.7–14.8 PBq (Aoyama et al., 2016b; Tsubono et al., 2016) and  $3.5 \pm 0.7$  PBq (Tsumune et al., 2012, 2013), respectively. The FNPP1-derived  $^{137}\text{Cs}$  inventory in the North Pacific Ocean has been estimated to be 15.2–18.3 PBq by comparing the observed inventory with model simulation results (Aoyama et al., 2016b),  $15.3 \pm 2.6$  PBq by optimum interpolation analysis (Inomata et al., 2016) and  $16.1 \pm 1.4$  PBq by model simulation (Tsubono et al., 2016). According to the estimation by Kaeriyama et al. (2014), the amount of  $^{134}\text{Cs}$  in the STMW was approximately  $4.2 \pm 1.1$  PBq in 2012. The estimation by Kaeriyama et al. (2014) implies that the FNPP1-derived  $^{137}\text{Cs}$  transported into the SOJ from 2012 to 2016 accounted for 5.0 % of the FNPP1-derived  $^{137}\text{Cs}$  inventory in the STMW. Approximately 60 %–65 % of the total inflow of FNPP1-derived  $^{137}\text{Cs}$  in the SOJ was transported in 2015 and 2016. After entering the SOJ, the FNPP1-derived  $^{137}\text{Cs}$  followed different paths. The amounts of FNPP1-derived  $^{137}\text{Cs}$  transported along the eastern TWC (2.6 % of the FNPP1-derived  $^{137}\text{Cs}$  inventory in the STMW) and western TWC (2.1 % of the FNPP1-derived  $^{137}\text{Cs}$  inventory in the STMW) were similar or slightly larger along the former path. Of the FNPP1-derived  $^{137}\text{Cs}$  transported in the SOJ, approximately 43 % returned to the North Pacific Ocean through the Tsugaru Strait during 2012–2016.

Because 5 % of the FNPP1-derived  $^{137}\text{Cs}$  in the STMW was transported into the SOJ, 95 % may remain in the STMW. On the basis of long-term measurements of the  $^{137}\text{Cs}$  activity concentration adjacent to the FNPP1, Tsumune et al. (2017) have estimated that the rate of direct release of FNPP1-derived  $^{137}\text{Cs}$  was  $2.2 \times 10^{14}$  Bq day $^{-1}$  until November 2011, after which it decreased exponentially with time to  $3.9 \times 10^9$  Bq day $^{-1}$  on 26 October 2015. Assuming that the rate of decrease in the  $^{137}\text{Cs}$  activity concentrations remained the same from 26 October 2015 to 31 December 2016, the total amount of  $^{137}\text{Cs}$  directly released from the FNPP1 site during the period 2012–2016 has been estimated to be 0.03 PBq (Tsumune et al., 2017). However, not all of the directly released  $^{137}\text{Cs}$  was subducted into the STMW. An amount equal to 0.03 PBq corresponds to 0.7 % of  $^{137}\text{Cs}$  inventory in the STMW. We can conclude that the FNPP1-derived  $^{137}\text{Cs}$  in STMW was decreasing during the study period.

An analysis of historical data from 1950 to 2000 indicates that the  $^{137}\text{Cs}$  activity concentrations in the western North Pacific Ocean were decreasing exponentially during that time. However, the  $^{137}\text{Cs}$  activity concentrations during 2000–2010 were almost constant at  $1.5\text{--}2$  Bq m $^{-3}$  (Inomata et al., 2009). Considering that there was scarcely any global fallout-derived  $^{137}\text{Cs}$  deposition after the 1970s, the  $^{137}\text{Cs}$  activity concentrations in the seawater of the North Pacific Ocean were controlled by physical oceanographic processes such as advection and diffusion from roughly 1980 until the FNPP1 accident (Inomata et al., 2009). Several studies have reported that there were subsurface maxima of  $^{137}\text{Cs}$  derived from global fallout in layers corresponding to surfaces of constant  $\sigma_\theta$  in the STMW and CMW (e.g. Aoyama et al., 2008). A possible explanation for the constancy of  $^{137}\text{Cs}$  activity concentrations during 2000–2010 is that the  $^{137}\text{Cs}$  subducted into the STMW and CMW in the 1960s might have returned to the surface after a few decades. However, the increase in FNPP1-derived  $^{137}\text{Cs}$  activity concentrations in the SOJ began in 2012–2013. This increase implies the existence of a faster transport route from the North Pacific Ocean to the SOJ via the subtropical gyre.

## 5 Conclusions

The  $^{137}\text{Cs}$  activity concentrations in the Sea of Japan (SOJ) increased beginning in 2012–2013 and reached a maximum in 2015–2016 of approximately 3 Bq m $^{-3}$ , which is above the pre-Fukushima accident level of 1.5 Bq m $^{-3}$ . The  $^{134}\text{Cs}/^{137}\text{Cs}$  activity ratios of 0.36–0.51 in the ECS and the SOJ are evidence that the increase in the  $^{137}\text{Cs}$  activity concentration was derived from the Fukushima accident.

An increase in FNPP1-derived  $^{137}\text{Cs}$  activity concentrations was first observed in the subsurface layer with a  $\sigma_\theta$  of  $\sim 25.2$  kg m $^{-3}$  (corresponding to STMW) in the southern part of the Kuroshio Current in the NPSJ in 2012–2013. The  $^{137}\text{Cs}$  activity concentrations in the NPSJ have been decreasing since 2014. In the ECS, an increase in FNPP1-derived  $^{137}\text{Cs}$  was observed in 2014; decreases have been observed since 2016. Vertical distributions of the  $^{137}\text{Cs}$  activity concentrations in the ECS were almost constant or contained a subsurface peak. These results indicated that there was a 1–2-year time lag between the maxima of  $^{137}\text{Cs}$  activity concentrations in the NPSJ and ECS. The increase in the  $^{137}\text{Cs}$  activity concentrations in the SOJ began in 2012 and continued until 2016. A time lag in the propagation of FNPP1-derived  $^{137}\text{Cs}$  of approximately 1 year was observed in the SOJ. The similarity of  $^{134}\text{Cs}/^{137}\text{Cs}$  activity ratios in the surface layers of the ECS, SOJ and Ogasawara region suggest that the source of radiocaesium was the same in all three of these regions.

The total amount of recirculated FNPP1-derived  $^{137}\text{Cs}$  from 2012 to 2016 was estimated to be  $0.21 \pm 0.01$  PBq, which corresponds to 5.0 % of the FNPP1-derived  $^{137}\text{Cs}$  in

the STMW. Of this total, the amounts of FNPP1-derived  $^{137}\text{Cs}$  transported along the western and eastern TWC were almost the same or slightly larger along the eastern TWC. Of the FNPP1-derived  $^{137}\text{Cs}$  transported into the SOJ, approximately 43 % (2.1 % of the total amount in STMW) passed through the Tsugaru Strait and back into the North Pacific Ocean. The FNPP1-derived  $^{137}\text{Cs}$  transported northwards was estimated to be 14 % of the amount transported into the SOJ (0.7 % of the total amount in STMW).

The most important result of this study was the determination that FNPP1-derived  $^{137}\text{Cs}$  was rapidly transported into the SOJ within several years after the FNPP1 accident.

**Data availability.** Most of the data before the FNPP1 accident are included in the database Historical Artificial Radionuclides in the Pacific Ocean and its Marginal Seas (HAM database) (Aoyama and Hirose, 2004, and their updated version). The data recorded after the FNPP1 accident have been presented by Aoyama et al. (2016a). The Japanese government's monitoring data are reported by the Marine Ecology Research Institute (<http://www.kaiseiken.or.jp/publish/itaku/itakuseika.html>, in Japanese). The Korean government monitoring data are reported by the Korea Institute of Nuclear Safety ([http://clean.kins.re.kr/info/in03\\_rept\\_list.jsp](http://clean.kins.re.kr/info/in03_rept_list.jsp), in Korean).

**Supplement.** The supplement related to this article is available online at: <https://doi.org/10.5194/os-14-813-2018-supplement>.

**Author contributions.** YI (corresponding author) conducted data analysis and the preparation of the manuscript with contributions from all co-authors. MA developed the database of radioactivity and pretreatment of seawater samples for measurement of radiocaesium. YH measured the radiocaesium activity concentrations. MY organized the seawater sampling for radiocaesium measurement.

**Competing interests.** The authors declare that they have no conflict of interest.

**Acknowledgements.** For collection of seawater samples, the authors thank Miyuki Takahashi and Shun-pei Tomita of the Oga Aquarium, Akita, Japan; the staff at Kinosaki Aquarium, Hyogo, Japan; Hajime Chiba at Toyama Kosen, Toyama, Japan; Shigeo Takeda and the captain and crew of the *Nagasaki-maru*, Nagasaki Univ.; Mitsuru Hayashi and the captain and crew of the *Fukae-maru* Kobe Univ.; Yuki Nikaido and the crew of the Sado Kisen, Niigata, Japan; Akira Wada and the captain and crew of the ferry *Queen Coral Plus* of the Marix Line, Kagoshima, Japan; Kenichi Sasaki and the captain and crew of the *Ushio-maru*, Hokkaido Univ., Hakodate, Japan; and Keiri Imai and the captain and crew of the *Oshoro-maru*, Hokkaido Univ., Hakodate, Japan. We thank Eitarou Oka of the University of Tokyo and an anonymous reviewer for valuable comments. We also thank Naoki Hirose of Kyusyu University for providing us with seawater volume

transport data. We also thank Rika Hozumi for her work extracting radiocaesium from seawater samples. This research was financially supported by a Grant-in-Aid for Scientific Research on Innovative Areas, “Interdisciplinary study on environmental transfer of radionuclides from the Fukushima Dai-ichi NPP Accident” (project no. 25110511) from the Japanese Ministry of Education, Culture, Sports, Science and Technology (MEXT). This research was also supported with funds provided by the cooperation program of the Institute of Nature and Environmental Technology, Kanazawa University (JFY2016, 2017), and the cooperation program of the Institute of Radiation Emergency Medicine, Hirosaki University (JFY2016, 2017).

Edited by: Matthew Hecht

Reviewed by: Eitarou Oka and one anonymous referee

## References

- Aoyama, M.: Oceans and Seas, in: Radionuclides in the Environment, Jon Wiley & Sons, West Sussex, UK, 339–345, 2010.
- Aoyama, M. and Hirose, K.: Artificial Radionuclides database in the Pacific Ocean: HAM database, *Sci. World J.*, 4, 200–215, 2004.
- Aoyama, M. and Hirose, K.: Radiometric determination of anthropogenic radionuclides in seawater, in: Radioactivity in the Environment, 11, Elsevier, Oxford, UK, 137–162, 2008.
- Aoyama, M., Hirose, K., and Igarashi, Y.: Re-construction and updating our understanding on the global weapons tests  $^{137}\text{Cs}$  fallout, *J. Environ. Monit.*, 8, 431–438, 2006.
- Aoyama, M., Hirose, K., Nemoto, K., Takatsuki, Y., and Tsumune D.: Water masses labeled with global fallout  $^{137}\text{Cs}$  formed by subduction in the North Pacific, *Geophys. Res. Lett.*, 35, L01604, <https://doi.org/10.1029/2007GL031964>, 2008.
- Aoyama, M., Tsumune, D., and Hamajima, Y.: Distribution of  $^{137}\text{Cs}$  and  $^{134}\text{Cs}$  in the North Pacific Ocean: impacts of the TEPCO Fukushima-Daiichi NPP accident, *J. Radioanal. Nucl. Ch.*, 296, 535–539, 2013a.
- Aoyama, M., Uematsu, M., Tsumune, D., and Hamajima, Y.: Surface pathway of radioactive plume of TEPCO Fukushima NPP1 released  $^{134}\text{Cs}$  and  $^{137}\text{Cs}$ , *Biogeosciences*, 10, 3067–3078, <https://doi.org/10.5194/bg-10-3067-2013>, 2013b.
- Aoyama, M., Hamajima, Y., Hult, M., Uematsu, M., Oka, E., Tsumune, D., and Kumamoto, Y.:  $^{134}\text{Cs}$  and  $^{137}\text{Cs}$  in the North Pacific Ocean derived from the March 2011 TEPCO Fukushima Dai-ichi Nuclear Power Plant accident, Japan. Part one: surface pathway and vertical distributions, *J. Oceanogr.*, 72, 53–65, 2016a.
- Aoyama, M., Kajino, M., Tanaka, T. Y., Sekiyama, T. T., Tsumune, D., Tsubono, T., Hamajima, Y., Inomata, Y., and Gamo, Y.:  $^{134}\text{Cs}$  and  $^{137}\text{Cs}$  in the North Pacific Ocean derived from the March 2011 TEPCO Fukushima Dai-ichi Nuclear Power Plant accident, Japan. Part two: estimation of  $^{134}\text{Cs}$  and  $^{137}\text{Cs}$  inventories in the North Pacific Ocean, *J. Oceanogr.*, 72, 67–76, 2016b.
- Aoyama, M., Hamajima, Y., Inomata, Y., and Oka, E.: Recirculation of FNPP1-derived radiocaesium observed in winter 2015/2016 in coastal regions of Japan, *Appl. Radiat. Isot.*, 126, 83–87, 2017.
- Buesseler, K., Aoyama, M., and Fukasawa, M.: Impacts of Fukushima Nuclear Power Plants on Marine Radioactivity, *Environ. Sci. Technol.*, 45, 9931–9935, 2011.

- Buesseler, K., Dai, M., Aoyama, M., Benitez-Nelson, C., Charms-son, S., Higley, K., Maderich, V., Masque, P., Oughton, D., and Smith, J. N.: Fukushima Daiichi-Derived Radionuclides in the Ocean: Transport, Fate, and Impacts, *Annu. Rev. Mar. Sci.*, 9, 1–31, 2016.
- Budyansky, M. V., Goryachev, V. A., Kaplunenko, D. D., Lobanov, V. B., Prants, S. V., Sergeev, A. F., Shlyk, N. V., and Uleysky, M. Y.: Role of mesoscale eddies in transport of Fukushima-derived cesium isotopes in the ocean, *Deep-Sea Res. Pt. I*, 96, 15–27, 2015.
- Fukudome, K., Yoon, J.-H., Ostrovskii, A., Takikawa, T., and Han, I.-S.: Seasonal volume transport variation in the Tsushima warm current through the Tsushima Straits from 10 Years of ADCP Observations, *J. Oceanogr.*, 66, 539–551, 2010.
- Hamajima, Y. and Komura, K.: Background components of Ge detectors in Ogoya underground laboratory, *Appl. Radiat. Isot.* 61, 179–183, 2004.
- Han, S., Hirose, N., Usui, N., and Miyazawa, Y.: Multi-model ensemble estimation of volume transport through the straits of the East/Japan Sea, *Ocean Dynam.*, 66, 59–76, 2016.
- Hirose, K.: Fukushima Daiichi Nuclear Plant accident: Atmospheric and oceanic impacts over the five years, *J. Environ. Radioactiv.*, 157, 113–130, 2016.
- Honda, M. C., Aono, T., Aoyama, M., Hamajima, Y., Kawakami, H., Kitamura, M., Masumoto, Y., Miyazawa, Y., Takigawa, M., and Saino, T.: Dispersion of artificial caesium-134 and-137 in the western North Pacific one month after the Fukushima accident, *Geochem. J.*, 46, e1–e9, 2012.
- Inomata, Y., Aoyama, M., and Hirose, K.: Record of surface  $^{137}\text{Cs}$  concentrations in the global ocean using the HAM-global database, *J. Environ. Monit.*, 11, 116–125, 2009.
- Inomata, Y., Aoyama, M., Tsumune, D., Motoi, T., and Nakano, H.: Optimum interpolation analysis of basin-scale  $^{137}\text{Cs}$  transport in surface seawater in the North Pacific Ocean, *J. Environ. Monit.*, 14, 3146–3155, 2012.
- Inomata, Y., Aoyama, M., Tsubono, T., Tsumune, D., and Hirose, K.: Spatial and temporal distributions of  $^{134}\text{Cs}$  and  $^{137}\text{Cs}$  derived from the TEPCO Fukushima Daiichi Nuclear Power Plant accident in the North Pacific Ocean by using optimal interpolation analysis, *Environ. Sci.*, 18, 126–136, 2016.
- Inoue, M., Kofuji, H., Nagao, S., Yamamoto, M., Hamajima, Y., Yoshida, K., Fujimoto, K., Takada, T., and Isoda, Y.: Lateral variation of  $^{134}\text{Cs}$  and  $^{137}\text{Cs}$  concentrations in surface seawater in and around the Japan Sea after the Fukushima Dai-ichi Nuclear Power Plant accident, *J. Environ. Radioactiv.*, 109, 45–51, 2012.
- Kaeriyama, H., Ambe, D., Shimizu, Y., Fujimoto, K., Ono, T., Yonezaki, S., Kato, Y., Matsunaga, H., Minami, H., Nakatsuka, S., and Watanabe, T.: Direct observation of  $^{134}\text{Cs}$  and  $^{137}\text{Cs}$  in surface seawater in the western and central North Pacific after the Fukushima Dai-ichi nuclear power plant accident, *Biogeosciences*, 10, 4287–4295, <https://doi.org/10.5194/bg-10-4287-2013>, 2013.
- Kaeriyama, H., Shimizu, Y., Ambe, D., Masujima, M., Shigenobu, Y., Fujimoto, K., Ono, T., Nishiuchi, K., Taneda, T., and Kurogi, H.: Southwest intrusion of  $^{134}\text{Cs}$  and  $^{137}\text{Cs}$  derived from the Fukushima Dai-ichi Nuclear Power Plant accident in the Western North Pacific, *Environ. Sci. Technol.*, 48, 3120–3127, 2014.
- Kaeriyama, H., Shimizu, Y., Setou, T., Kumamoto, Y., Okazaki, M., Ambe, D., and Ono, T.: Intrusion of Fukushima-derived radiocaesium into subsurface water due to formation of mode waters in the North Pacific, *Sci. Rep.*, 6, 22010, <https://doi.org/10.1038/srep22010>, 2016.
- Kamidaira, Y., Uchiyama, Y., Kawamura, H., Kobayashi, T., and Furuno, A.: Submesoscale Mixing on Initial Dilution of Radionuclides Released From the Fukushima Daiichi Nuclear Power Plant, *J. Geophys. Res.*, 123, 2808–2828, 2018.
- Kodama, T., Igeta, Y., Kuga, M., and Abe, S.: Long-term decrease in phosphate concentrations in the surface layer of the southern Japan Sea, *J. Geophys. Res.*, 121, 7845–7856, 2016.
- Korea Institute of Nuclear Safety: Marine Environmental Radioactivity Survey, available at: [http://clean.kins.re.kr/info/in03\\_rept\\_list.jsp](http://clean.kins.re.kr/info/in03_rept_list.jsp) (last access: 17 August 2018), 2011 (in Korean).
- Korea Institute of Nuclear Safety: Marine Environmental Radioactivity Survey, available at: [http://clean.kins.re.kr/info/in03\\_rept\\_list.jsp](http://clean.kins.re.kr/info/in03_rept_list.jsp) (last access: 17 August 2018), 2012 (in Korean).
- Korea Institute of Nuclear Safety: Marine Environmental Radioactivity Survey, available at: [http://clean.kins.re.kr/info/in03\\_rept\\_list.jsp](http://clean.kins.re.kr/info/in03_rept_list.jsp) (last access: 17 August 2018), 2013 (in Korean).
- Korea Institute of Nuclear Safety: Marine Environmental Radioactivity Survey, available at: [http://clean.kins.re.kr/info/in03\\_rept\\_list.jsp](http://clean.kins.re.kr/info/in03_rept_list.jsp) (last access: 17 August 2018), 2014 (in Korean).
- Korea Institute of Nuclear Safety: Marine Environmental Radioactivity Survey, available at: [http://clean.kins.re.kr/info/in03\\_rept\\_list.jsp](http://clean.kins.re.kr/info/in03_rept_list.jsp) (last access: 17 August 2018), 2015 (in Korean).
- Korea Institute of Nuclear Safety: Marine Environmental Radioactivity Survey, available at: [http://clean.kins.re.kr/info/in03\\_rept\\_list.jsp](http://clean.kins.re.kr/info/in03_rept_list.jsp) (last access: 17 August 2018), 2016 (in Korean).
- Kumamoto, Y., Murata, A., Kawano, T., and Aoyama, M.: Fukushima-derived radiocesium in the northwestern Pacific Ocean in February 2012, *Appl. Radiat. Isot.*, 81, 335–339, 2013.
- Kumamoto, Y., Aoyama, M., Hamajima, Y., Aono, T., Kouketsu, S., Murata, A., and Kawano, T.: Southward spreading of the Fukushima-derived radiocesium across the Kuroshio Extension in the North Pacific, *Sci. Rep.*, 4, 4276, <https://doi.org/10.1038/srep04276>, 2014.
- Kumamoto, Y., Aoyama, M., Hamajima, Y., Murata, and A., and Kawano, T.: Impact of Fukushima-derived radiocesium in the western North Pacific Ocean about ten month after the Fukushima Dai-ichi nuclear power plant accident, *J. Environ. Radioactiv.*, 140, 114–122, 2015.
- Kumamoto, Y., Aoyama, M., Hamajima, Y., Nagai, H., Yamagata, T., Kawai, Y., Oka, E., Yamaguchi, A., Imai, K., and Murata, A.: Fukushima-derived radiocesium in the western North Pacific in 2014, *J. Radioanal. Nucl. Ch.*, 311, 1209–1217, 2017.
- Marine Ecology Research Institute: Radiation level survey in marine organizations and their environment, available at: <http://www.kaiseiken.or.jp/publish/itaku/itakuseika.html> (last access: 17 August 2018), 2011 (in Japanese).
- Marine Ecology Research Institute: Radiation level survey in marine organizations and their environment, available at: <http://www.kaiseiken.or.jp/publish/itaku/itakuseika.html> (last access: 17 August 2018), 2012 (in Japanese).
- Marine Ecology Research Institute: Radiation level survey in marine organizations and their environment, available at: <http://www.kaiseiken.or.jp/publish/itaku/itakuseika.html> (last access: 17 August 2018), 2013 (in Japanese).
- Marine Ecology Research Institute: Radiation level survey in marine organizations and their environment, available at: <http://www.kaiseiken.or.jp/publish/itaku/itakuseika.html> (last access: 17 August 2018), 2013 (in Japanese).

- [//www.kaiseiken.or.jp/publish/itaku/itakuseika.html](http://www.kaiseiken.or.jp/publish/itaku/itakuseika.html) (last access: 17 August 2018), 2014 (in Japanese).
- Marine Ecology Research Institute: Radiation level survey in marine organizations and their environment, available at: <http://www.kaiseiken.or.jp/publish/itaku/itakuseika.html> (last access: 17 August 2018), 2015 (in Japanese).
- Marine Ecology Research Institute: Radiation level survey in marine organizations and their environment, available at: <http://www.kaiseiken.or.jp/publish/itaku/itakuseika.html> (last access: 17 August 2018), 2016 (in Japanese).
- Menard, H. W. and Smith, M.: Hypsometry of ocean basin provinces, *J. Geophys. Res.*, 71, 4305–4325, 1966.
- Masuzawa, J.: Subtropical Mode Water, *Deep-Sea Res.*, 16, 463–472, 1969.
- Miyao, T., Hirose, K., Aoyama, M., and Igarashi, Y.: Temporal Variation of  $^{137}\text{Cs}$  and  $^{239,240}\text{Pu}$  in the Sea of Japan, *J. Environ. Radioactiv.*, 40, 239–250, 1998.
- Nishida, Y., Kanomata, I., Tanaka, I., Sato, S., Takahashi, S., and Matsubara, H.: Seasonal and interannual variations of the volume transport through the Tsugaru Strait, *Oceanography in Japan*, 12, 487–499, 2003.
- Oka, E.: Seasonal and interannual variation of North Pacific Subtropical Mode Water in 2003–2006, *J. Oceanogr.*, 65, 151–164, 2009.
- Oka, E. and Qiu, B.: Progress of North Pacific mode water research in the past decade, *J. Oceanogr.*, 68, 5–20, <https://doi.org/10.1007/s10872-011-0032-5>, 2012.
- Oka, E., Qiu, B., Kouketsu, S., Uehara, K., and Suga, T.: Decadal seesaw of the Central and Subtropical Mode Water formation associated with the Kuroshio Extension variability, *J. Oceanogr.*, 68, 355–360, 2012.
- Prants, S. V., Ponomarev, V. I., Budyansky, M. V., Yu, M., Uleysky, M. Yu., and Fyman, P. A.: Lagrangian analysis of the vertical structure of eddies simulated in the Japan Basin of the Japan/East Sea, *Ocean Modell.*, 86, 128–140, <https://doi.org/10.1016/j.ocemod.2014.12.010>, 2015.
- Rossi, V., Van Sebille, E., Sen Gupta, A., Garçon, V., and England, M. H.: Multi-decadal projections of surface and interior pathways of the Fukushima Cesium-137 radioactive plume, *Deep-Sea Res. Pt. I*, 80, 37–46, 2013.
- Tsubono, T., Misumi, K., Tsumune, D., Bryan, F.O., Hirose, K., and Aoyama, M.: Evaluation of radioactive cesium impact from atmospheric deposition and direct release fluxes into the North Pacific from the Fukushima Daiichi nuclear power plant, *Deep-Sea Res. Pt. I*, 115, 10–21, 2016.
- Tsumune, D., Tsubono, T., Aoyama, M., and Hirose, K.: Distribution of oceanic  $^{137}\text{Cs}$  from the Fukushima Dai-ichi Nuclear Power Plant simulated numerically by a regional ocean model, *J. Environ. Radioactiv.*, 111, 100–108, 2012.
- Tsumune, D., Tsubono, T., Aoyama, M., Uematsu, M., Misumi, K., Maeda, Y., Yoshida, Y., and Hayami, H.: One-year, regional-scale simulation of  $^{137}\text{Cs}$  radioactivity in the ocean following the Fukushima Dai-ichi Nuclear Power Plant accident, *Biogeosciences*, 10, 5601–5617, <https://doi.org/10.5194/bg-10-5601-2013>, 2013.
- Tsumune, F., Aoyama, M., Hirose, K., Tsubono, T., Misumi, K., and Tateda, Y.: Estimation of direct release rate of  $^{137}\text{Cs}$ ,  $^{90}\text{Sr}$  and  $^3\text{H}$  from the Fukushima Dai-ichi Nuclear Power Plant for four-and-a-half years, in: *Proceedings of the 4th International Conference on Environmental Radioactivity*, Vilnius, Lithuania, 29 May–2 June 2017, 24–28, 2017.